Published in final edited form as:
J Infect Dis. 2010 November 1; 202(9): 1415–1423. doi:10.1086/656534.

Tissue Factor-Dependent Procoagulant Activity of Subtilase Cytotoxin, a Potent AB_5 Toxin Produced by Shiga Toxigenic *Escherichia coli*

Hui Wang[1], **James C. Paton**[1], **Cheleste M. Thorpe**[2], **Claudine S. Bonder**[3], **Wai Yan Sun**[3], and **Adrienne W. Paton**[1]

[1] Research Centre for Infectious Diseases, School of Molecular and Biomedical Science, University of Adelaide, S.A., 5005, Australia

[2] Division of Geographic Medicine and Infectious Diseases, Tufts-New England Medical Center, Boston, MA, 02111, USA

[3] Centre for Cancer Biology, SA Pathology and School of Medicine, University of Adelaide, Adelaide, S.A., 5000, Australia

Abstract

Subtilase cytotoxin (SubAB), produced by certain virulent Shiga toxigenic *Escherichia coli* strains, causes hemolytic uremic syndrome-like pathology in mice, including extensive microvascular thrombosis. SubAB acts by specifically cleaving the essential endoplasmic reticulum chaperone BiP. BiP has been reported to inhibit the activation of tissue factor (TF), the major initiator of extrinsic coagulation. We hypothesised that the apparent prothrombotic effect of SubAB in vivo may involve the stimulation of TF-dependent procoagulant activity (PCA). TF-dependent PCA, TF mRNA levels and BiP cleavage were therefore examined in human macrophage (U937) cells and primary human umbilical vein endothelial cells (HUVECs) exposed to SubAB. In both U937s and HUVECs SubAB significantly increased TF-dependent PCA, induced TF mRNA expression and mediated BiP cleavage. No effects were seen when cells were treated with a non-proteolytic mutant toxin $SubA_{A272}B$. Our results suggest that the procoagulant effect of SubAB may be dependent on both the up-regulation of TF expression as well as the activation of TF via BiP cleavage.

Keywords

subtilase cytotoxin; Shiga toxin; tissue factor; coagulation; BiP

INTRODUCTION

Shiga toxigenic *Escherichia coli* (STEC) cause serious gastrointestinal disease in humans, which can lead to the potentially fatal hemolytic uremic syndrome (HUS). HUS is characterized by a triad of microangiopathic hemolytic anemia, thrombocytopenia and renal failure, believed to be principally caused by Shiga toxin (Stx)-mediated damage to the microvascular endothelium [1]. Interestingly, some STEC strains produce an unrelated AB_5 toxin called subtilase cytotoxin (SubAB) [2]. These STEC lack the locus of enterocyte effacement (LEE),

Reprints or correspondence: Adrienne W. Paton, School of Molecular and Biomedical Science, University of Adelaide, S.A., 5005, Australia (adrienne.paton@adelaide.edu.au).

The authors declare that there are no potential conflicts of interest.

which is thought to contribute to the virulence of the better characterized O157:H7 strains. Although SubAB-positive STEC are less common than LEE-positive strains, they are nevertheless capable of causing severe human disease, including outbreaks of HUS [2,3]. Remarkably, intraperitoneal injection of purified SubAB causes HUS-like pathology in mice, including extensive microvascular thrombosis and other histological damage in the brain, kidneys and liver, as well as a dramatic splenic atrophy [4]. These findings raise the possibility that SubAB directly contributes to pathology in humans infected with strains of STEC that produce both Shiga toxin and SubAB.

SubAB acts by binding to glycan receptors on the surface of target cells via its B pentamer, followed by internalization and retrograde transport to the endoplasmic reticulum (ER) [5]. Once in the ER compartment, its A subunit (an extraordinarily specific subtilase-like serine protease) cleaves an essential ER Hsp70 family chaperone called binding immunoglobulin protein (BiP) [6]. BiP (also known as 78-kDa glucose regulated protein [GRP78]) is responsible for proper folding of newly synthesized proteins, and as the master regulator of the ER stress response, it is essential for maintenance of ER homeostasis [7]. Previous studies have shown that over-expression of BiP in T24/83 cells, a prothrombotic human bladder carcinoma cell line, decreases thrombin generation by inhibiting cell surface tissue factor (TF) procoagulant activity (PCA), thereby suppressing the prothrombotic potential of the cells [8]. BiP has also been reported to negatively regulate TF PCA in both murine endothelial and macrophage cells via direct binding to and functional inhibition of TF [9]. TF is a 47-kDa transmembrane glycoprotein, and is the major physiological initiator of the extrinsic coagulation cascade. TF binds to the serine protease, factor VII/VIIa, leading to activation of factors IX and X and the subsequent generation of thrombin [10]. TF is implicated in many pathological conditions including atherosclerosis [11], post-operative thrombosis [12], sepsis-linked disseminated intravascular coagulation [13,14], chronic inflammation [15] and cancer [16]. Alternatively spliced human tissue factor (asTF) is a soluble isoform of TF present in blood, which may also contribute to procoagulant activity [17,18]. Both TF and asTF have been detected in many cell types including macrophages and endothelial cells [9,18].

Since SubAB cleaves BiP and BiP is known to inhibit activation of TF on the surface of many cell types, we hypothesised that the apparent prothrombotic effect of SubAB observed in vivo may involve stimulation of TF-dependent PCA. In this study, we examined TF PCA by measuring TF-dependent factor Xa (FXa) generation and compared the effects of SubAB and Shiga toxin 2 (Stx2) in human macrophage (U937) cells and primary human umbilical vein endothelial cells (HUVECs). We also investigated BiP cleavage, as well as TF and asTF gene expression in cells exposed to SubAB.

METHODS

Purification of toxin

SubAB and its non-toxic derivative ($SubA_{A272}B$) were purified as described previously [2, 16]. This involved fusion of a His_6 tag to the C-terminus of the B subunit, enabling purification by Ni-NTA chromatography under non-denaturing conditions. Stx2 was purified using an identical approach.

Cell culture and toxin treatment

All cells were grown at 37°C in 5% CO_2, in culture medium (RPMI 1640 medium supplemented with 10 mM HEPES, 0.2 M L-Glutamine, 10% heat-inactivated FCS, and 50 IU of penicillin and 50 μg of streptomycin per ml). U937 cells were kindly provided by Michael James, Rheumatology Unit, Royal Adelaide Hospital. HUVECs were harvested and cultured as described previously [20]. HUVECs were used at passage 4 or less. For toxin treatment,

cells were seeded into appropriately sized tissue culture plates, 1–2 × 10^6 U937 cells per ml or confluent monolayers of HUVECs were exposed to SubAB, $SubA_{A272}B$ or Stx2 at the indicated concentrations in culture medium containing 1% heat-inactivated FCS for the indicated times.

Cell-based tissue factor dependent factor Xa generation assay

In a 24-well culture plate, U937 cells (≈10^6 cells/well) or HUVECs (confluent monolayer) were incubated with toxins at indicated concentrations in 260 μl of culture medium containing 1% FCS without phenol red at 37°C in 5% CO_2 for 1, 4, 6, 16 or 24 h. Factor VIIa (10 nmol/L, Enzyme Research Laboratories, HFVIIa 2793AL) and Factor X (50 nmol/L, Enzyme Research Laboratories, HFX 2942AL) were then added and trays were incubated at 37°C for a further 30 min. Reactions were stopped by adding 100 mmol/L EDTA and the supernatants were transferred to flat bottom 96-well plates (Maxisorp Nunc-Immuno plates; Nunc, Roskilde, Denmark). The chromogenic substrate Spectrozyme FXa (0.75 mM, American Diagnostics, Cat# 222) was added to the supernatants and incubated for 30 minutes at 37°C in the dark. Theactivity of the generated FXa in the medium was quantified by the Absorbance at 405 nm, using a SpectroMax M2 Microplate reader and Soft Max software (Molecular Devices, USA).

RNA extraction

RNA was extracted from approximately 10^7 toxin-treated U937 cells or HUVECs using a RNeasy Mini Kit (Qiagen, Germany) according to the manufacturer's instructions. RNasin RNase inhibitor (Promega) was then added to the samples. Contaminating DNA was digested with RNase-free DNase I (Roche Molecular Diagnostics), followed by DNase stop solution (Promega). The absence of DNA contamination in all RNA preparations was confirmed by reverse transcription-PCR (RT-PCR) analysis using primers specific for the gene encoding the housekeeping enzyme glyceraldehyde-3-phosphate dehydrogenase (GAPDH). The gene encoding GAPDH contains an intron such that the mRNA template directs amplification of a 239-bp product, whereas the chromosomal DNA template directs amplification of a 341-bp product.

Real-time RT-PCR and RT-PCR

TF mRNA (Genbank NM_001993) is 2153 bp in length and includes 6 exons, whereas asTF mRNA lacks exon-5 (160 bp) [17]. The oligonucleotide primer pairs used in this study are as follows: TF (75-bp amplicon), GGGAATTCAGAGAAATATTCTACATCA and TAGCCAGGATGATGACAAGGA; asTF (78-bp amplicon), TCTTCAAGTTCAGGAAAGAAATATTCT and CCAGGATGATGACA AGGATGA; and GAPDH (239-bp amplicon), TCCTTGGAGGCCATGTGGGCCAT and TGATGACATCAAGAAGGTGGTGAAG. The comparative levels of TF mRNA and asTF mRNA were determined using quantitative real-time RT-PCR. RT-PCR was performed using a one-step Access RT-PCR system (Promega) according to the manufacturer's instructions. Each reaction was performed in a final volume of 20 μl containing 20 nmol of each oligonucleotide and a 1/50,000 dilution of SYBR Green I nucleic acid stain (BMA). The quantitative RT-PCR was performed on a Rotorgene RG-2000 cycler (Corbett Research, Mortlake, NSW, Australia) and included the following steps: 45 min of RT at 48°C followed by 2 min denaturation at 94°C and then 40 cycles of amplification at 94°C for 30 s, 56°C for 30 s, and 72°C for 45 s. Each RNA sample was assayed in triplicate using primers specific for TF and asTF mRNAs, or mRNA for GAPDH, which was used as an internal control. Results were calculated using the comparative cycle threshold ($2^{\Delta\Delta Ct}$) method (user bulletin no. 2 [http://docs.appliedbiosystems.com/pebiodocs/04303859.pdf]; Applied Biosystems), in which the amount of target mRNA is normalized to a reference (medium only control) relative to an internal control (GAPDH mRNA). Results are expressed as relative changes in TF and

asTF mRNA levels compared to medium only control levels. Standard deviations (SD) were initially determined according to the formula $SD = \sqrt{(SD\ of\ sample)^2 + (SD\ of\ GAPDH)^2}$, and the result was then applied to the formulae $+SD = 2^{\Delta\Delta Ct\text{-}SD} - 2^{\Delta\Delta Ct}$ and $-SD = 2^{\Delta\Delta Ct} - 2^{\Delta\Delta Ct + SD}$.

SDS-PAGE analysis and western immunoblotting

After toxin treatment, cells were harvested and resuspended in 2 × LUG (5% β-mercaptoethanol, 62.5 mM Tris-HCl, 2% SDS, 10% glycerol, 0.05% bromophenol blue, pH6.8). The culture supernatant was also collected, and incubated with 12.5% trichloroacetic acid (TCA) on ice for 1 hour. The TCA-precipitated proteins were centrifuged (24,000 × *g*, 30 min, 4°C), washed with acetone and then redissolved in 2 × LUG. Cell lysates or TCA-precipitated supernantant protein samples were boiled for 5 min and separated by SDS-polyacrylamide gel electrophoresis (SDS-PAGE) [21].

Protein samples separated on SDS-PAGE gels (13%) were electroblotted onto PVDF (Immobilon) or nitrocellulose membranes and probed with goat anti-human BiP/GRP78 (c-20, Santa Cruz Biotechnology). Labelled bands were detected using anti-goat IgG conjugated to alkaline phosphatase or HRP, with NBT/X-phosphate substrate (Roche) or chemiluminescent substrate (Sigma), respectively. Novex Sharp prestained protein ladder (Invitrogen) was used as molecular size marker.

Flow cytometry

To determine the time course of SubAB internalization in U937 cells, following SubAB treatment, U937 cells were washed and fixed in 1% paraformaldyhyde at indicated time points. After permeabilization with 0.1% Triton X-100, intracellular SubAB was labelled using rabbit anti-SubA followed by Alexa 488-conjugated anti-rabbit IgG (Invitrogen). After 4 PBS washes, cell suspensions were subjected to FACS analysis; data from ten thousand cells for each sample were acquired using a FACSCanto, and analysed with CellQuest™ Pro software (Becton Dickinson).

Fluorescence microscopy

To determine the intracellular distribution of SubAB taken by HUVECs, cells were incubated for 1 h with SubAB (1 μg/ml), washed with ice cold PBS and kept on ice. SubAB was labelled with anti-SubA and Alexa 488-conjugate as described above. The cells were then washed and examined with an EVOS-fl high-resolution digital inverted fluorescence microscope system, and digital images were captured.

RESULTS

Internalization of SubAB by U937 cells and HUVECs

FACS analysis showed that SubAB was rapidly internalised by U937 cells, reaching a peak within 30 min of exposure to the toxin (Figure 1*A*). Fluorescence microscopy also demonstrated that a significant amount of SubAB was internalised by HUVECs after 1 h of incubation. SubAB taken up by HUVECs was seen in a large juxtanuclear region of the cytoplasm as well as in puncta (Figure 1*B*). Both the kinetics of SubAB uptake and its distribution within these cell types are consistent with that reported previously for Vero cells [5].

SubAB-mediated BiP cleavage

Western blot analysis showed significant BiP cleavage in SubAB-treated U937 cells (Figure 2*A*) as well as in HUVECs (Figure 2*B*). This was evident from reduced levels of the native 72-

kDa protein and appearance of a 28-kDa C-terminal fragment (the other BiP cleavage product, a 44-kDa N-terminal fragment [6] is not seen because the antibody used is specific for a peptide derived from the C-terminus). No BiP cleavage was detected in cells treated with a mutant toxin ($SubA_{A272}B$) [2], which lacks protease activity (data not shown) or in cells treated with Stx2 (Figure 2). Cleavage of BiP in SubAB-treated cells was apparent at the earliest time points tested (30 and 60 min for U937s [Figure 2*A*] and HUVECs, [figure 2*B*], respectively). Furthermore, the cleaved 28-kDa C-terminal BiP fragment was detected in the cell lysate as well as in the culture medium (supernatant) from both U937 cells and HUVECs. However, the native BiP (72-kDa) was not detected in the supernatant from HUVECs (Figure 2).

Tissue factor mRNA induction

RT-PCR studies showed that TF and asTF are expressed in both U937 cells and HUVECs. Real-time RT-PCR analysis showed that both SubAB and Stx2 increased TF and asTF mRNA levels in U937 cells. Maximal up-regulation of both isoforms (2–3-fold for TF and 3–4-fold for asTF) occurred at 1 h in cells exposed to either SubAB or Stx2 (Figure 3). The response of HUVECs to SubAB was slower, but much more profound, with maximal up-regulation (approximately 18-fold and 9-fold for TF and asTF mRNA, respectively) occurring 4 hours after toxin treatment. Interestingly, however, the response of HUVECs to Stx2 was much lower, not exceeding 2.2-fold up-regulation for either isoform at any time point (Figure 3).

Procoagulant activity

SubAB induced significant increases in tissue factor-dependent FXa generation in U937 cells (Figure 4). The procoagulant effect of SubAB was both dose- and time-dependent, with maximal stimulation occurring at 4–6 h (Figure 4). Stx2 also stimulated tissue factor-dependent FXa generation in U937 cells to a similar extent, and with similar kinetics (Figure 5*A* and *B*). Interestingly, there was no evidence of pro-coagulant synergy between SubAB and Stx2. Responses were not significantly greater in U937 cells treated with a combination of SubAB and Stx2 (both used at doses of either 0.1 or 0.01 μg/ml) compared with those treated with either toxin alone (Fig. 5*B*). The basal level of tissue factor-dependent FXa generation elicited by un-treated U937 cells, and that elicited by cells treated with either SubAB or Stx2, was significantly higher when cells were assayed rather than the respective culture supernatants (Fig. 6). This indicates that the toxin-induced PCA is largely attributable to activation of cell membrane-bound TF rather than the soluble as TF.

Tissue factor-dependent FXa generation was also stimulated by treatment of HUVECs with either SubAB or Stx2. However, the time course was delayed markedly relative to that in U937s. Statistically significant stimulation was not observed before 6 h and maximal stimulation of procoagulant activity occurred at 16–24 h (Figure 7). For both SubAB and Stx2, PCA responses were significantly greater than control cells from 6–48 h. At the 6, 16 and 24 h time points, SubAB elicited significantly stronger procoagulant responses than Stx2. However, the response elicited by Stx2 was still maintained at its maximal level at 48 h, at which time it was significantly greater than that elicited by SubAB. The non-proteolytic $SubA_{A272}B$ did not elicit significant TF-dependent PCA relative to untreated HUVECs at any time point (Figure 7).

DISCUSSION

This study demonstrated that SubAB as well as Stx2 significantly increases TF-dependent PCA in both human macrophages and endothelial cells. The procoagulant effect of SubAB appeared and peaked earlier in macrophages than in HUVECs, although the maximal levels achieved were similar. Real time RT-PCR results showed that TF and asTF are expressed in both cell types, which is consistent with previous findings in murine and human cells [9,18].

Furthermore, TF and asTF mRNAs were up-regulated by SubAB and Stx2 in both cell lines. The induction of TF and asTF mRNAs in U937 cells was detected earlier than that observed in HUVECs, which is consistent with the earlier onset of toxin-induced TF-dependent PCA in U937s. However, the fold-increases in mRNA levels for both TF and asTF in SubAB- or Stx2-treated HUVECs were much greater and were sustained for a much longer time than those in similarly-treated U937s. This apparent discrepancy between the extent of gene up-regulation and actual TF-dependent PCA responses in the two cell types could be explained by lower baseline TF and asTF mRNA levels in HUVECs relative to U937s, such that absolute post-induction mRNA levels are similar. The findings are also consistent with a significant proportion of the PCA response being due to release/activation of pre-existing TF.

Previous studies have shown that TF expression and its PCA is increased by exposure to lipopolysacharide (LPS) [22–24]. However, in the present study, we used toxins purified from a *lpxM*-negative recombinant *E. coli* host strain, the LPS of which has negligible endotoxic activity. Moreover, TF-dependent PCA was not induced by treatment with the non-proteolytic $SubA_{A272}B$, which was purified under identical conditions to SubAB and Stx2. Thus, the effects seen in this study are not due to contaminating endotoxin.

The absence of TF-dependent PCA in cells treated with $SubA_{A272}B$ also indicates that proteolytic cleavage of the ER chaperone BiP, (the only known substrate of SubAB [6]) is essential for the phenomenon. BiP has been shown to negatively regulate TF PCA in both cell-based and non cell-based coagulation assays [8,9]. The inhibitory effect was not mediated by a decrease in cell surface TF protein levels, suggesting that retention of TF in the ER or attenuation of TF synthesis are not responsible [8]. Pozza and Austin have proposed that BiP inhibits TF activation either directly by formation of a BiP-TF complex, locking TF into a latent or encrypted conformation, or indirectly by sequestering intracellular calcium and attenuating apoptotis [25]. In the present study, the former seems a more likely explanation, as significant SubAB-dependent TF-PCA responses are evident by 4 h and 6 h for U937s and HUVECs, respectively, which is too rapid for an apoptosis-dependent mechanism. In Vero cells, which are highly susceptible to SubAB, apoptosis is not evident until approximately 30 h [26], and for U937s, significant apoptosis is not seen until 48 h (our unpublished data). In contrast, cleavage of BiP occurs rapidly in SubAB-treated U937 and HUVEC cells, and this may directly trigger dissociation of BiP-TF complexes. SubAB-mediated BiP cleavage may also contribute to TF-dependent PCA indirectly through downstream effects on cellular signalling pathways. The toxin rapidly induces an unfolded protein response in Vero cells by activation of the PKR-like ER kinase (PERK), inositol-requiring enzyme 1 (IRE1), and activating transcription factor 6 (ATF6) ER stress signalling pathways [26]. It is also known to induce proinflammatory cytokine responses by activation of NF-κB via phosphorylation of Akt in rat renal epithelial cells [27]. Proinflammatory cytokines have previously been shown to augment cell surface TF activity following exposure of human glomerular endothelial cells to Stx [28]. Thus, SubAB may share certain mechanisms with Stx in the up-regulation of TF-dependent PCA. However, the capacity of SubAB to cleave BiP and thereby directly mediate release/activation of cell-surface TF is a prothombotic mechanism unique to this novel cytotoxin.

In summary, SubAB as well as Stx2 significantly increase TF-dependent PCA in human macrophages and endothelial cells in vitro. Both toxins are similarly effective, but do not appear to exert a synergistic effect at the doses tested. The procoagulant effect of SubAB may be dependent not only on the up-regulation of TF expression, but also on BiP-cleavage-dependent activation of pre-existing TF. Disturbance of the coagulation cascade may be critically important in triggering HUS in humans. TF-dependent FXa generation activates thrombin, which in turn increases fibrin deposition and platelet aggregation, leading to thrombotic microangiopathy and thrombocytopenia. Moreover, deposition of fibrin clots in glomerular

capillaries leads to renal insufficiency, as well as physical damage to erythrocytes. This triad of microangiopathic hemolytic anemia, thrombocytopenia and renal failure is the defining hallmark of HUS. We have previously reported that intraperitoneal injection of purified SubAB induces HUS-like pathology in mice; there was extensive microvascular thrombosis, haemolytic anemia, thrombocytopenia and renal insufficiency, as well as extensive ischaemic damage to multiple organs including the kidneys, liver and brain [4]. Thus, SubAB-mediated stimulation of TF-dependent PCA may directly contribute to thrombotic microangiopathy in patients with HUS caused by gastrointestinal infection with SubAB-producing STEC strains.

Acknowledgments

Supported by Project Grant 565359 and Program Grant 565526 from the National Health and Medical Research Council of Australia (NHMRC) and R01AI-068715 from the National Institutes of Health, USA. JCP is a NHMRC Australia Fellow.

References

1. Paton JC, Paton AW. Pathogenesis and diagnosis of Shiga toxin-producing *Escherichia coli* infections. Clin Microbiol Rev 1998;11:450–479. [PubMed: 9665978]
2. Paton AW, Srimanote P, Talbot UM, Wang H, Paton JC. A new family of potent AB_5 cytotoxins produced by Shiga toxigenic *Escherichia coli*. J Exp Med 2004;200:35–46. [PubMed: 15226357]
3. Paton AW, Woodrow MC, Doyle RM, Lanser JA, Paton JC. Molecular characterization of a Shiga-toxigenic *Escherichia coli* O113:H21 strain lacking *eae* responsible for a cluster of cases of hemolytic-uremic syndrome. J Clin Microbiol 1999;37:3357–3361. [PubMed: 10488206]
4. Wang H, Paton JC, Paton AW. Pathologic changes in mice induced by subtilase cytotoxin, a potent new *Escherichia coli* AB_5 toxin that targets the endoplasmic reticulum. J Infect Dis 2007;196:1093–101. [PubMed: 17763334]
5. Chong DC, Paton JC, Thorpe CM, Paton AW. Clathrin-dependent trafficking of subtilase cytotoxin, a novel AB_5 toxin that targets the endoplasmic reticulum chaperone BiP. Cell Microbiol 2008;10:795–806. [PubMed: 18042253]
6. Paton AW, Beddoe T, Thorpe CM, et al. AB_5 subtilase cytotoxin inactivates the endoplasmic reticulum chaperone BiP. Nature 2006;443:548–452. [PubMed: 17024087]
7. Lee AS. The glucose-regulated proteins: stress induction and clinical applications. Trends Biochem Sci 2001;26:504–510. [PubMed: 11504627]
8. Watson LM, Chan AK, Berry LR, et al. Overexpression of the 78-kDa glucose-regulated protein/immunoglobulin-binding protein (GRP78/BiP) inhibits tissue factor procoagulant activity. J Biol Chem 2003;278:17438–17447. [PubMed: 12621026]
9. Bhattacharjee G, Ahamed J, Pedersen B, et al. Regulation of tissue factor--mediated initiation of the coagulation cascade by cell surface grp78. Arterioscler Thromb Vasc Biol 2005;25:1737–1743. [PubMed: 15947236]
10. Ruf W, Edgington TS. Structural biology of tissue factor, the initiator of thrombogenesis in vivo. FASEB J 1994;8:385–390. [PubMed: 8168689]
11. Tremoli E, Camera M, Toschi V, Colli S. Tissue factor in atherosclerosis. Atherosclerosis 1999;144:273–283. [PubMed: 10407489]
12. Miller CL, Graziano C, Lim RC, Chin M. Generation of tissue factor by patient monocytes: correlation to thromboembolic complications. Thromb Haemost 1981;46:489–495. [PubMed: 7302886]
13. Levi M. The coagulant response in sepsis and inflammation. Hamostaseologie 2010;30:10–16. [PubMed: 20162247]
14. Osterud B, Flaegstad T. Increased tissue thromboplastin activity in monocytes of patients with meningococcal infection: related to an unfavourable prognosis. Thromb Haemost 1983;49:5–7. [PubMed: 6845273]
15. Nakagomi A, Sasaki M, Ishikawa Y, et al. Upregulation of monocyte tissue factor activity is significantly associated with low-grade chronic inflammation and insulin resistance in patients with metabolic syndrome. Circ J 2010;74:572–577. [PubMed: 20103969]

16. Kasthuri RS, Taubman MB, Mackman N. Role of tissue factor in cancer. J Clin Oncol 2009;27:4834–4838. [PubMed: 19738116]

17. Bogdanov VY, Balasubramanian V, Hathcock J, Vele O, Lieb M, Nemerson Y. Alternatively spliced human tissue factor: a circulating, soluble, thrombogenic protein. Nature Med 2003;9:458–462. [PubMed: 12652293]

18. Szotowski B, Antoniak S, Poller W, Schultheiss HP, Rauch U. Procoagulant soluble tissue factor is released from endothelial cells in response to inflammatory cytokines. Circ Res 2005;96:1233–1239. [PubMed: 15920023]

19. Talbot UM, Paton JC, Paton AW. Protective immunization of mice with an active-site mutant of subtilase cytotoxin of Shiga toxin-producing *Escherichia coli*. Infect Immun 2005;73:4432–4436. [PubMed: 15972544]

20. Litwin M, Clark K, Noack L, et al. Novel cytokine-independent induction of endothelial adhesion molecules regulated by platelet/endothelial cell adhesion molecule (CD31). J Cell Biol 1997;139:219–228. [PubMed: 9314541]

21. Laemmli UK. Cleavage of structural proteins during the assembly of the head of bacteriophage T4. Nature 1970;227:680–685. [PubMed: 5432063]

22. Erlich J, Fearns C, Mathison J, Ulevitch RJ, Mackman N. Lipopolysaccharide induction of tissue factor expression in rabbits. Infect Immun 1999;67:2540–2546. [PubMed: 10225918]

23. Brutzki TC, Kulczycky MJ, Bardossy L, Clarke BJ, Blajchman MA. Rapid in vivo induction of leukocyte tissue factor mRNA and protein synthesis following low dose endotoxin administration to rabbits. Hematol J 2001;2:188–195. [PubMed: 11920244]

24. Sugatani J, Igarashi T, Munakata M, et al. Activation of coagulation in C57BL/6 mice given verotoxin 2 (VT2) and the effect of co-administration of LPS with VT2. Thromb Res 2000;100:61–72. [PubMed: 11053618]

25. Pozza LM, Austin RC. Getting a GRP on tissue factor activation. Arterioscler Thromb Vasc Biol 2005;25:1529–1531. [PubMed: 16055754]

26. Wolfson J, Thorpe CM, May KL, et al. Subtilase cytotoxin activates PERK, ATF6 and IRE1 endoplasmic reticulum stress-signaling pathways. Cell Microbiol 2008;10:1775–1786. [PubMed: 18433465]

27. Yamazaki H, Hiramatsu N, Hayakawa K, et al. Activation of the Akt - NF-κB pathway by subtilase cytotoxin through the ATF6 branch of the unfolded protein response. J Immunol 2009;183:1480–1487. [PubMed: 19561103]

28. Nestoridi E, Tsukurov O, Kushak RI, Ingelfinger JR, Grabowski EF. Shiga toxin enhances functional tissue factor on human glomerular endothelial cells: implications for the pathophysiology of hemolytic uremic syndrome. J Thromb Haemost 2005;3:752–762. [PubMed: 15842359]

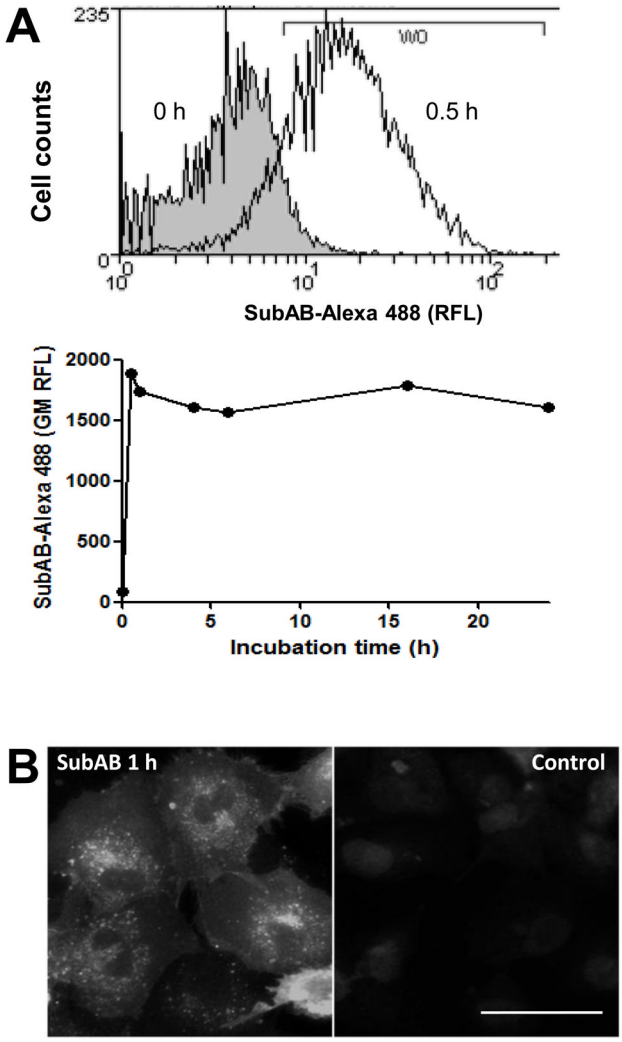

Figure 1.

Internalization of SubAB by U937 cells and HUVECs. Cells were incubated with 1μg/ml of SubAB at 37°C for the indicated times. Cells were fixed, permeabilized and probed with rabbit anti-SubAB followed by antirabbit-Alexa 488 conjugate. *A*, FACS analysis of SubAB internalization in U937 cell: upper panel, histogram showing SubAB positive cells (defined by histogram marker W0) detected after 0 or 0.5 h of incubation; lower panel, time course of SubAB internalization (expressed as geometric mean relative fluorescence intensity; GM RFI). *B*, fluorescence image of SubAB internalized by HUVECs at 1 h (scale bar is 50 μm).

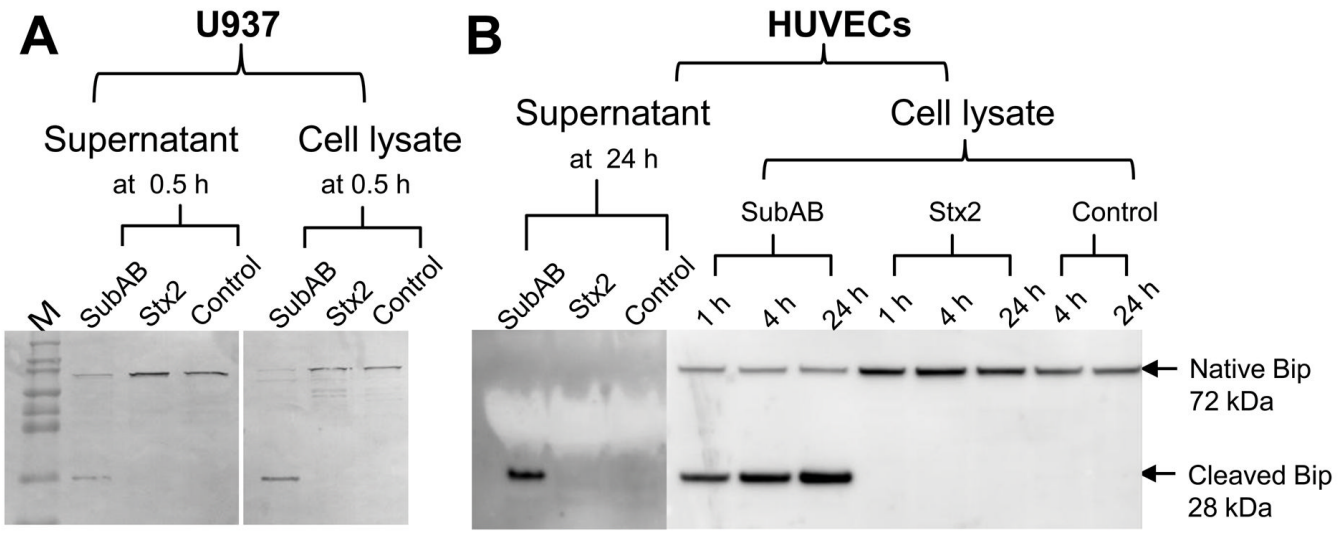

Figure 2.

SubAB-mediated BiP cleavage in U937 cells *(A)* and HUVECs *(B)*. Cells were exposed to SubAB or Stx2 at 1 μg/ml for the indicated times. Cell lysate or supernatant proteins were separated, electroblotted, and probed with anti-BiP as described in the Methods. The mobilities of immunoreactive native BiP (72 kDa) and the cleaved C-terminal fragment (28 kDa) are indicated. M denotes molecular size markers (Novex Sharp Protein Standards; Invitrogen).

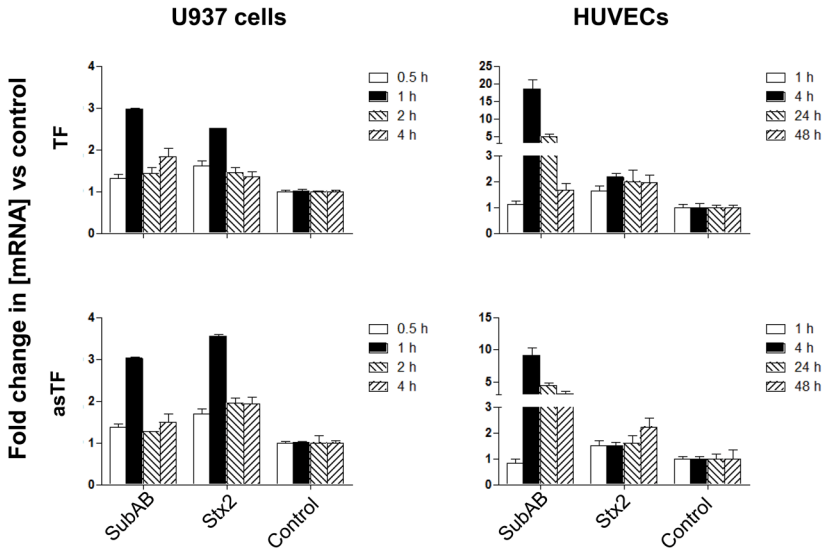

Figure 3.

Induction of TF and asTF mRNA by SubAB and Stx2. RNA was isolated from U937 cells or HUVECs treated with 1 μg/ml of SubAB or Stx2 for the indicated times. TF and asTF mRNA was measured using quantitative real time RT-PCR. Results are expressed as the fold change in [mRNA] relative to that in control (medium only) cells, and data shown are the mean ± SD for triplicate assays.

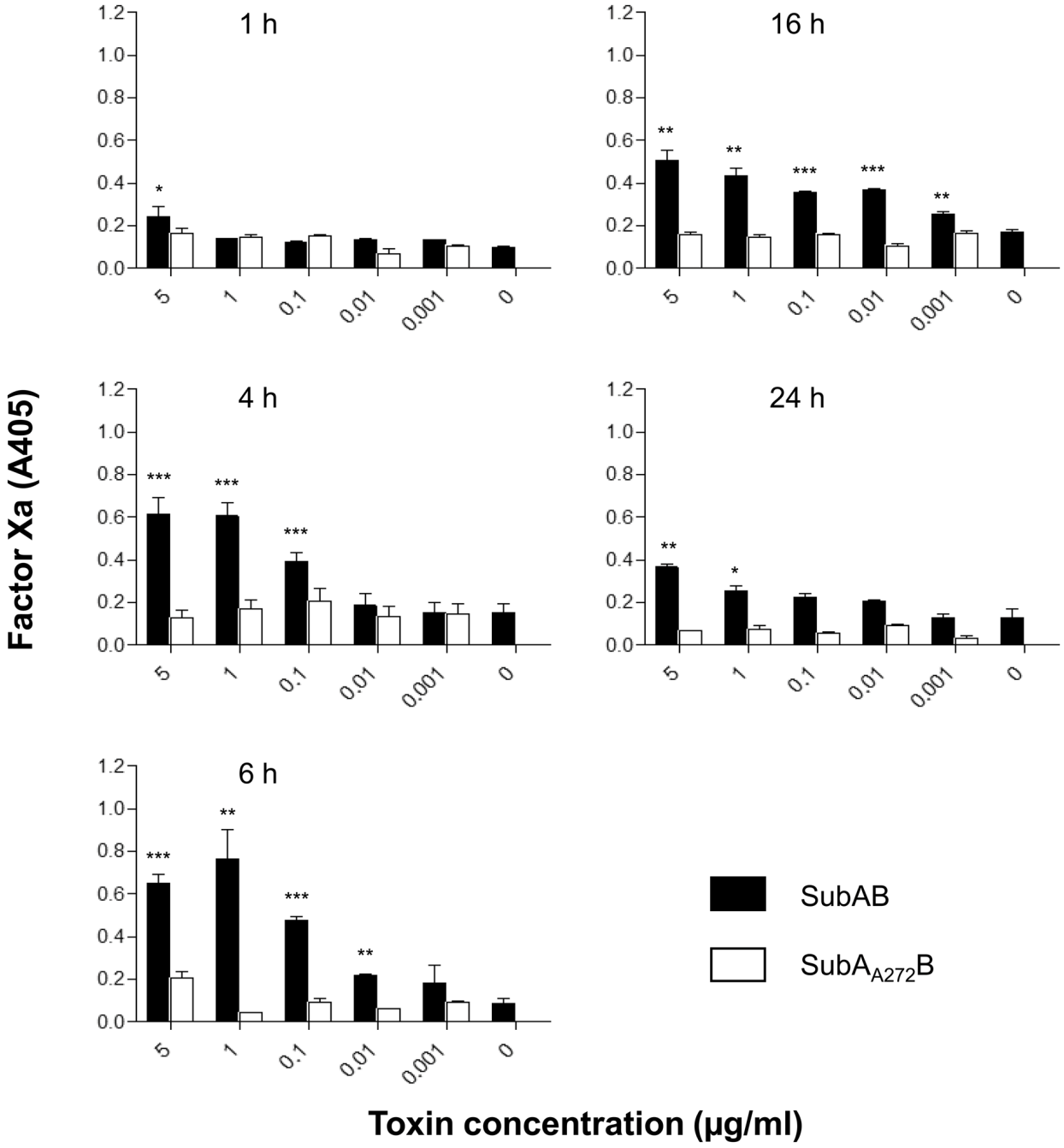

Figure 4.

Stimulation of TF-dependent factor Xa generation in U937 cells. U937 cells were incubated with SubAB or its non-toxic derivative (SubA$_{A272}$B) at the indicated concentrations for 1–24 h. Factor Xa generation was quantified using chromogenic substrate and A_{405} was read as described in the Methods. Data shown are the mean ± standard error of the mean (SEM) from triplicate assays. The differences between SubAB and SubA$_{A272}$B treated cells were analyzed using Student's *t* test: ***$P < 0.001$; **$P < 0.01$; *$P < 0.05$.

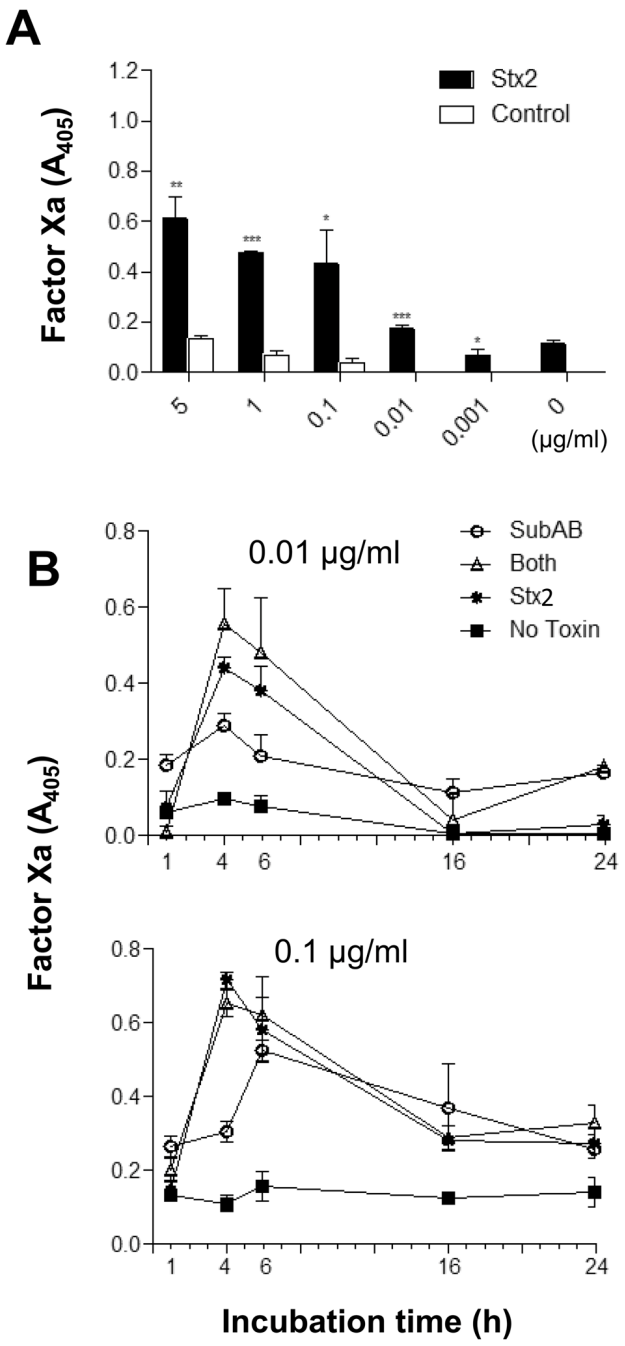

Figure 5.

Comparison of the procoagulant effects of SubAB and Stx2. U937 cells were incubated with SubAB or Stx2 at indicated concentrations for various times. *A*, dose-response of the effect of Stx2 on TF-dependent Factor Xa generation at 4 h. *B*, time courses of TF-dependent Factor Xa generation by U937 cells treated with low doses of SubAB and Stx2, alone and in combination. Factor Xa generation was quantified using chromogenic substrate and A_{405} was read as described in the Methods. Data shown are the mean ± SEM from triplicate assays. The differences between Stx2 treated cells and control cells were analyzed using Student's *t* test: ***$P < 0.001$; **$P < 0.01$; *$P < 0.05$.

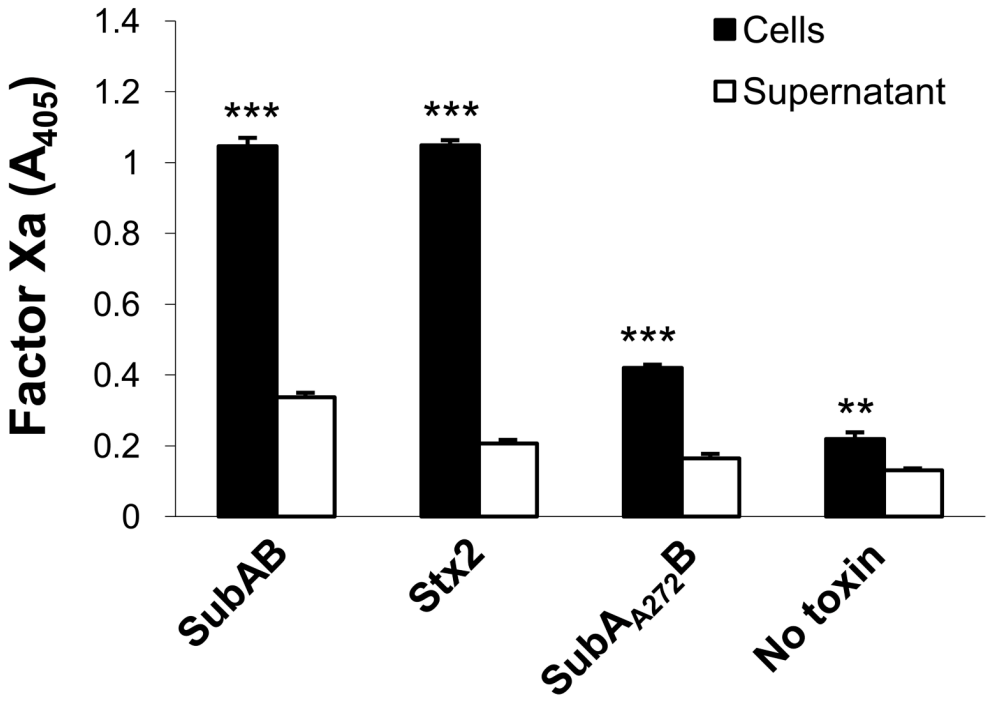

Fig. 6.

Comparison of TF-dependent factor Xa generation in cells and the culture medium. U937 cells were incubated with 1 μg/ml of SubAB, $SubA_{A272}B$ or Stx2 for 4 h. Cells and culture medium (supernatant) fractions were then separated and assayed for Factor Xa generation as described in the Methods. Data shown are the mean ± SEM from triplicate assays. The differences in Factor Xa generation between cell and supernatant fractions were analyzed using Student's *t* test: ***$P < 0.001$; **$P < 0.01$.

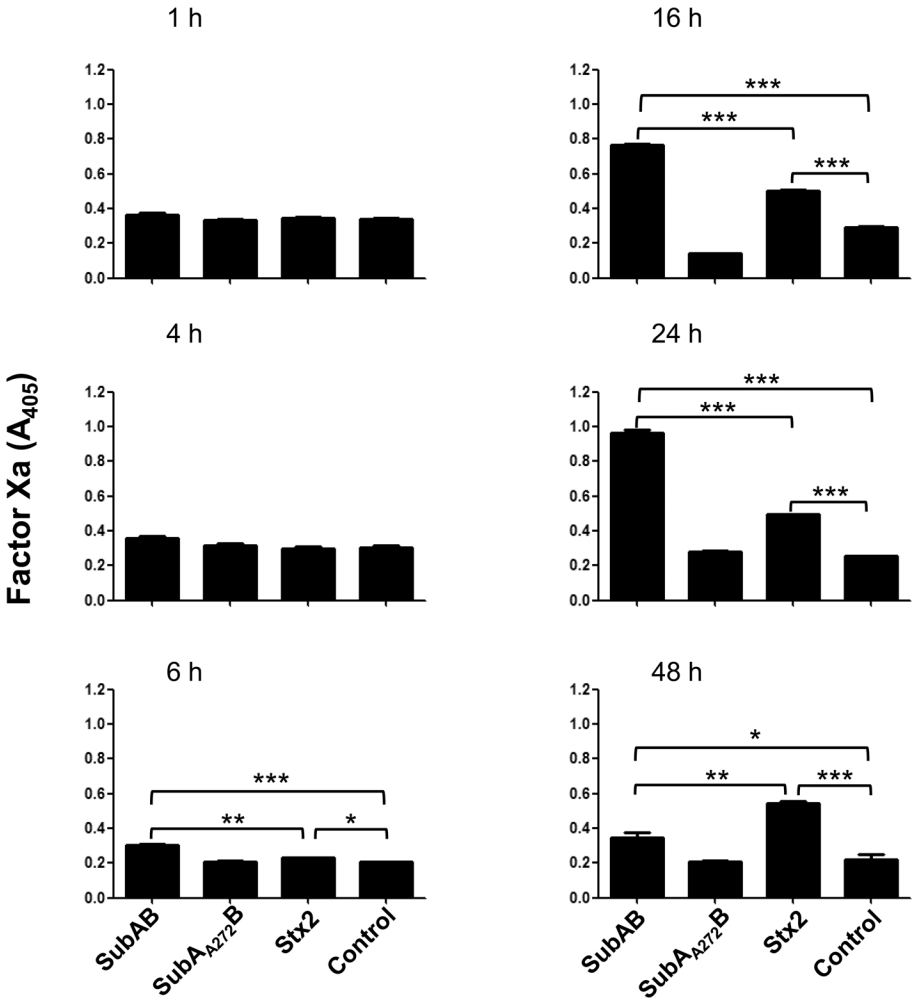

Figure 7.

Stimulation of TF-dependent factor Xa generation in HUVECs. HUVECs were incubated with 1 μg/ml SubAB, $SubA_{A272}B$, Stx2, or medium only (control) for 1–48 h. Factor Xa generation was quantified using chromogenic substrate as described in the Methods. Data shown are the mean ± SEM from triplicate assays. The differences between treatments indicated by the horizontal square were analyzed using Student's *t* test: ***$P < 0.001$; **$P < 0.01$; *$P < 0.05$.